

# Low energy $\gamma$ - $\gamma$ and $e^-$ - $\gamma$ PAC measurements using APDs and the probe nuclei $^{83}\text{Rb}$ ( $^{83}\text{Kr}$ ) and $^{83\text{m}}\text{Kr}$ ( $^{83}\text{Kr}$ )

M. Arenz<sup>1</sup> · R. Vianden<sup>1</sup>

Published online: 31 October 2016  
© Springer International Publishing Switzerland 2016

**Abstract** In the field of Perturbed Angular Correlation (PAC) measurements Avalanche Photo Diodes (APD) are rarely used, despite their favourable properties for fast counting purposes at low energies. This work demonstrates their application in combination with a simple and cheap custom build voltage sensitive preamplifier module. Using the PAC nuclei  $^{83}\text{Rb}$ ( $^{83}\text{Kr}$ ) and  $^{83\text{m}}\text{Kr}$ ( $^{83}\text{Kr}$ ), the time resolution of the set-up is analysed and the feasibility of precise timing measurements is shown.

**Keywords** PAC · Perturbed angular correlation ·  $^{83}\text{Rb}$  ·  $^{83\text{m}}\text{Kr}$  · APD · Avalanche photo diode · Voltage sensitive amplifier

## 1 Introduction

In the last two decades, Avalanche Photo Diodes (APD) have become more common in experiments that involve the detection of low energy  $\gamma$  radiation and particles. The development of large-area devices with active areas as big as  $(10 \times 10) \text{ mm}^2$  available off the shelf have greatly increased the experimental possibilities. Low energy quanta can be detected directly, whereas scintillation crystals extend the application range to hundreds of keV for

---

This article is part of the Topical Collection on *Proceedings of the International Conference on Hyperfine Interactions and their Applications (HYPERFINE 2016), Leuven, Belgium, 3–8 July 2016*  
Edited by Kristiaan Temst, Stefaan Cottenier, Lino M. C. Pereira and André Vantomme

---

✉ M. Arenz  
arenz@hiskp.uni-bonn.de

R. Vianden  
vianden@hiskp.uni-bonn.de

<sup>1</sup> Helmholtz-Institut für Strahlen- und Kernphysik, Universität Bonn, 53115, Bonn, Germany

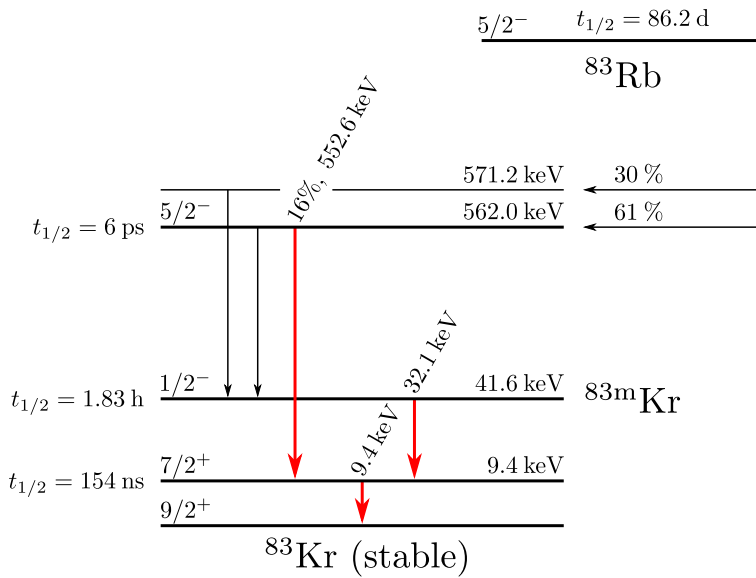


**Fig. 1** A simplified decay scheme of  $^{83}\text{Rb}$  taken from [3]. Both possible cascades, the  $\gamma$ - $\gamma$  and the  $e^-$ - $\gamma$  are shown in red

$\gamma$  radiation, all with good energy resolution [1]. Windowless APDs can be used to detect charged particles like conversion electrons directly with a high detection probability as well.

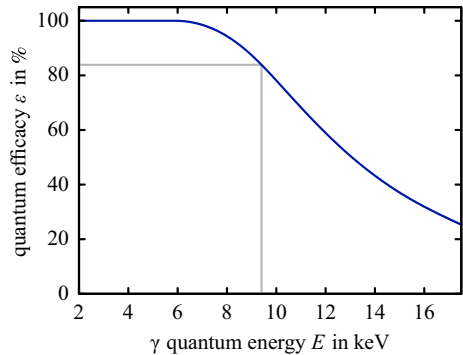
Furthermore, if used with an appropriate pre-amplifier, APDs show good timing properties. Depending on the active layer thickness and area, the time resolution can be in the range of some hundreds of ps [2]. The dead times of these detectors can be optimized to be in the ns regime, making them ideal candidates for fast counting applications.

Despite these favourable properties, APDs have rarely been used in the field of Perturbed Angular Correlation (PAC) measurements. Their application as low energy  $\gamma$  and conversion electron detector is discussed for the nuclei  $^{83}\text{Rb}$  ( $^{83}\text{Kr}$ ) and  $^{83\text{m}}\text{Kr}$  ( $^{83}\text{Kr}$ ).

The radionuclide  $^{83}\text{Rb}$  decays via an electron capture process with a half-life of  $t_{1/2} = 86.2(1)$  d [3]. This decay populates two cascades that pass through the same intermediate 9.4 keV level with  $7/2^+$  nuclear spin, a half-life of 155.1(12) ns [3] and a quadrupole moment of  $Q = 507(3)$  mb [4]. The first is a  $\gamma$ - $\gamma$  cascade consisting of a 553 keV and a 9.4 keV  $\gamma$  with an anisotropy coefficient of  $A_{22} = 0.06$ . The second one is an  $e^-$ - $\gamma$  cascade with the 17.8 keV K conversion electron of the 32.2 keV transition as start and the 9.4 keV  $\gamma$  as stop. Its anisotropy coefficient is  $A_{22} = -0.14$ . A simplified decay scheme with all relevant transitions and both cascades highlighted can be found in Fig. 1. Both cascades are good candidates for the application of the PAC method and can be measured simultaneously.

In contrast to the initial level's half-life of the first  $^{83}\text{Rb}$  ( $^{83}\text{Kr}$ ) cascade of 6.2(21) ps [3], the initial level of the second  $^{83}\text{Rb}$  ( $^{83\text{m}}\text{Kr}$ ) cascade is the isomeric  $^{83\text{m}}\text{Kr}$  level with a half-life of  $t_{1/2} = 1.83(2)$  h [3]. In the former case, the quadrupole interaction happens immediately after the decay of the parent and thus on the lattice site where  $^{83}\text{Rb}$  was incorporated after ion-implantation or an optional thermal treatment is examined. In the latter case, there is considerable time for interactions between probe nucleus and its environment. For instance, the noble gas  $^{83\text{m}}\text{Kr}$  may undergo diffusion processes during the half-life of the isomeric state. Hence, the interaction occurs on the lattice site of  $^{83\text{m}}\text{Kr}$ .

**Fig. 2** The quantum efficacy for the C30703FH-200T APD as provided by Excelitas. The value for 9.4 keV  $\gamma$  radiation is highlighted



## 2 Experimental details

To perform PAC measurements, the C30703FH-200T<sup>1</sup> reach-through APDs from Excelitas<sup>2</sup> are especially suited. These windowless devices with an active area of  $(10 \times 10)$  mm<sup>2</sup> feature a 200  $\mu$ m thick active layer, providing high quantum efficacies for the detection of low energy  $\gamma$  quanta, see Fig. 2. For <sup>83</sup>Rb(<sup>83</sup>Kr) and <sup>83m</sup>Kr(<sup>83</sup>Kr), the relevant 9.4 keV  $\gamma$  line and the 17.8 keV conversion electron are detected with a probability of roughly 84 % and 100 %, respectively. The signal rise time of this detector is specified as 5 ns.

To make use of the fast signals that APDs can provide, an appropriate amplifier has to be used. A design of a high-bandwidth ( $\lesssim 1$  GHz) voltage sensitive amplifier is given by Baron et al. [5]. However, the cited design is meant to be used at count rates exceeding 10 MHz and with detectors having thinner active layers and thus producing signals with rise times much shorter than the C30703FH-200T in question. For the purpose of PAC measurements, a reduction in bandwidth is facilitating the design of the circuit board without any drawbacks for the experiments.

The voltage sensitive preamplifier presented here is influenced by Baron et al. [5] and Flaxer [6] and consists of one MAR6+ input stage that is followed by two operation amplifiers that allow for an amplification adjustment. A circuit diagram is shown in Fig. 3.

The preamplifier is operated at a voltage gain of approximately 2000 and its bandwidth is in the range of 150 MHz, sample oscilloscope traces recorded using two detectors with different active layer thickness can be found in Fig. 4.

In the energy spectrum,  $\gamma$  quanta with energies above  $\sim 7$  keV have a tail towards lower energies that is more pronounced for higher energies. This is caused by radiation penetrating the avalanche region of the detector, causing incomplete charge carrier multiplication. This makes the determination of the energy resolution difficult, as it will vary over the detectable energy range. From recorded <sup>83</sup>Rb spectra (see Fig. 5), the energy resolution is estimated to be in the range of 20 % to 25 %. The lower detection threshold of this particular detector preamplifier combination is around 4.5 keV.

For the first measurements with the nucleus <sup>83</sup>Rb, a 100  $\mu$ m polycrystalline Be foil is ion implanted [7] with an implantation energy of 4 keV at the BONIS (BONn Isotope Separator) facility using activity produced as described by Vénos et al. [8]. In order to measure the

<sup>1</sup>Technical data on C30703FH-200T taken from C30703FH Avalanche Photodiode Interim Datasheet, Februar 2014 by Excelitas Technologies

<sup>2</sup>Formerly known as Perkin Elmer and EG&G

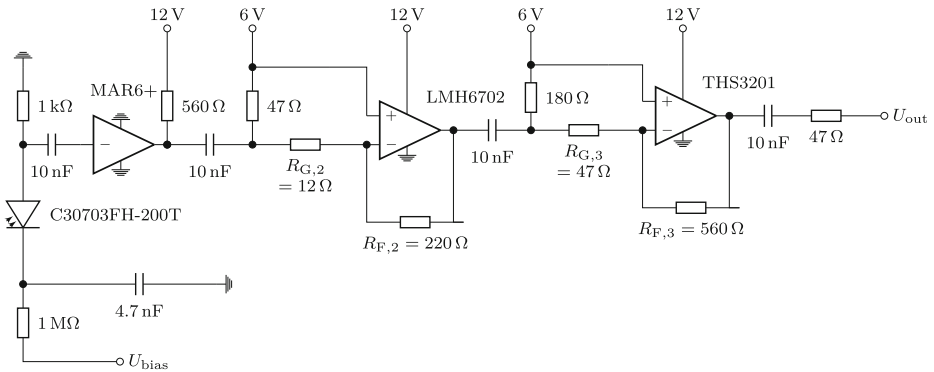


**Fig. 3** The amplifier circuit developed for PAC measurements. All resistors are thin film, only the 1 MΩ is a metal film resistor. All capacitors are of the C0G type, filter capacitors are omitted. The total amplification can be tuned using  $R_{G,i}$  and  $R_{F,i}$

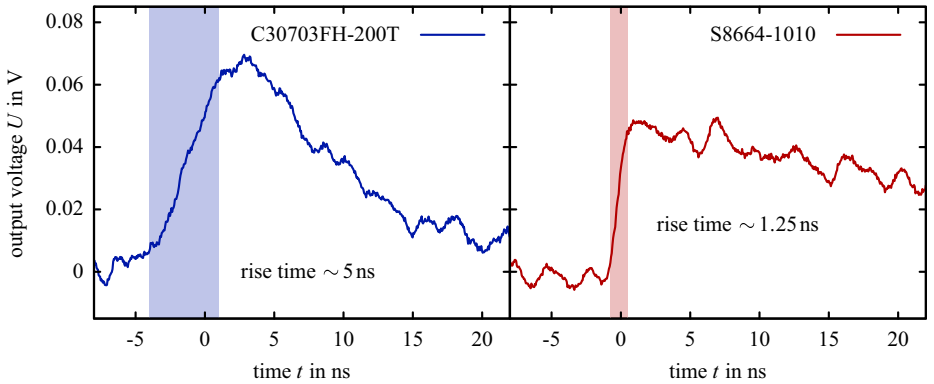


**Fig. 4** Typical oscilloscope traces produced with the present preamplifier module after the detection of a 12.6 keV X-ray. On the *left side* the output signal using a Excelitas C30703FH-200T detector as used for the measurements is shown. The rise time is limited by the detector and is in agreement with the value stated in the datasheet by Excelitas. On the *right side*, a signal produced with a much thinner APD, a Hamamatsu S8664-1010 is shown. Compared to the result of Baron et al. [2], in this case the preamplifier module limits the rise time

cascade involving 17.8 keV conversion electrons, the whole experiment has to be placed in vacuum. The measurement set-up’s backbone is a DN100 ConFlat six way cross. The vacuum pumps are connected from below, the sample is inserted from the top while four detectors, one scintillation detector and three avalanche photo diodes point towards the set-up’s centre from all four sides. The scintillation detector is a 2” × 2” CsF crystal. It is placed outside the vacuum in a hollow Al cylinder that is inserted into the six way cross from one side allowing for a positioning close to the sample. The additional 2 mm thin Al wall does not reduce the 553 keV  $\gamma$  intensity significantly.

When measuring with the described detector set-up, four spectra are obtained at the same time: a 90° and a 180° for both, the 553 keV–9.4 keV  $\gamma$ - $\gamma$  and the 17.8 keV–9.4 keV  $e^-$ - $\gamma$

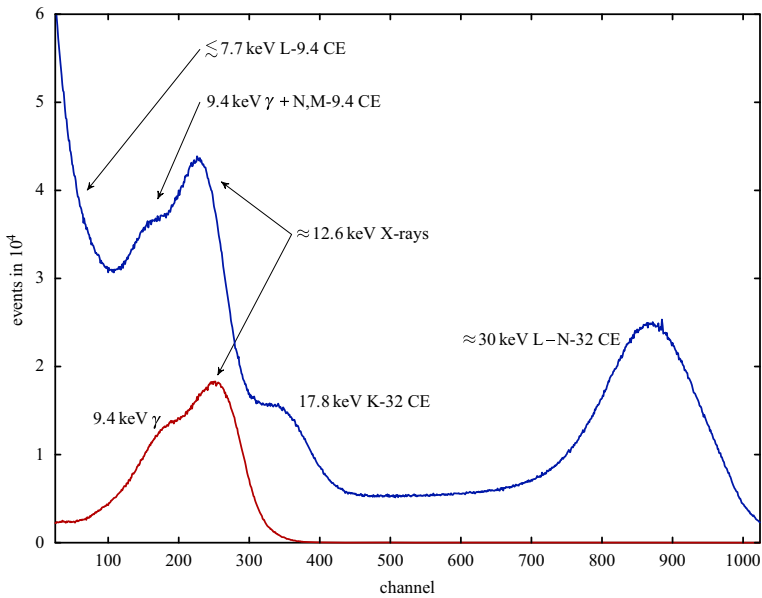


**Fig. 5** Energy spectra recorded with the APD and preamplifier with and without plastic foil absorber. The energy shift between both spectra is attributed to different intrinsic amplification of both diodes. The statistical uncertainties are too small to be shown in the plot

cascade. The APD that is used for the 17.8 keV start conversion electron can not be used as stop for the 553 keV–9.4 keV cascade. L, N and M conversion electrons from the 9.4 keV transition are not distinguishable from the  $\gamma$  line but are detected in the same detector. Due to the particle parameter, the anisotropies of a cascade stopped with the  $\gamma$  or with the corresponding conversion electron differ. For the other two detectors, a thin plastic foil that covers the APD’s active area prevents electrons from being detected, see Fig. 5.

### 3 Measurements

To prove a correct operation of the set-up, the half-life of the 9.4 keV intermediate level is determined using both available cascades in the decay of  $^{83}\text{Rb}$ . All four coincidence spectra that are measured simultaneously are shown in Fig. 6. The determined half-lives with fit uncertainties are  $\tau_{e-\gamma}^{180^\circ} = 155.9(3)$  ns,  $\tau_{e-\gamma}^{90^\circ} = 156.2(3)$  ns,  $\tau_{\gamma-\gamma}^{180^\circ} = 156.9(6)$  ns and  $\tau_{\gamma-\gamma}^{90^\circ} = 158.2(5)$  ns. All values agree with the literature value of 155.1(12) ns [3] if the uncertainty of the time calibration of 1 % is included.

The time resolution of the whole set-up can be determined by measuring the linewidth of simultaneous events in the time spectrum. The  $^{83}\text{Rb}$  decay provides such events for APD-only operation as well as for a mixed operation with a scintillation detector and an APD.

After the electron capture process has taken place, when the 553 keV–9.4 keV cascade is populated, a 12.6 keV X-ray is emitted. It is easily detected with the present set-up and

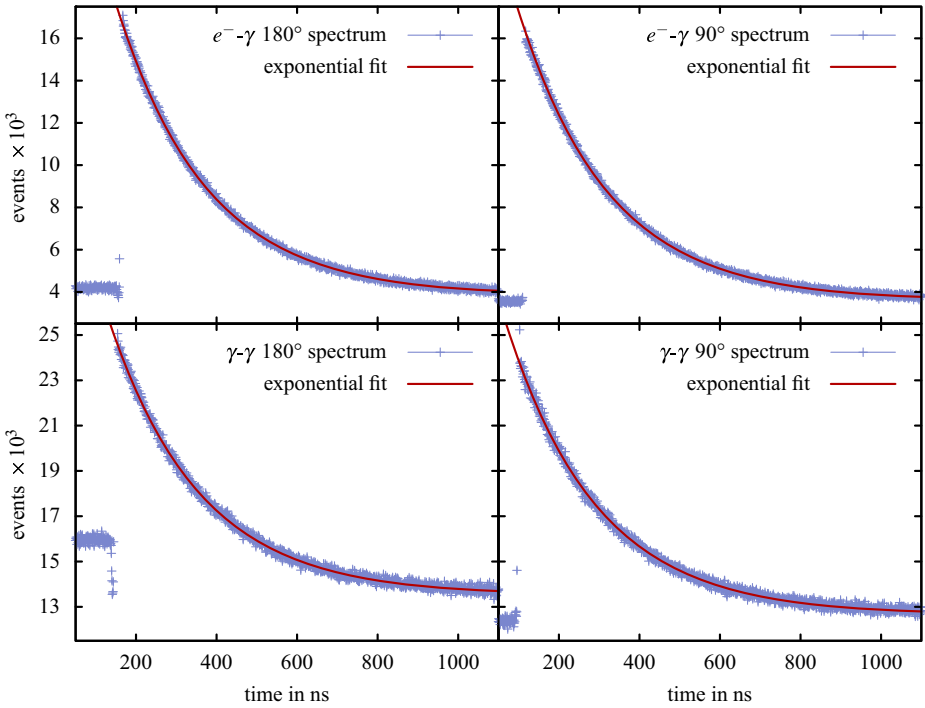


**Fig. 6** All recorded spectra, the top row shows  $e^- - \gamma$  spectra, the lower row  $\gamma - \gamma$  spectra. The routing glitch for  $t < 0$  in the  $180^\circ$   $\gamma - \gamma$  spectrum has no influence on the measurement. Statistical uncertainties are smaller than the data symbols

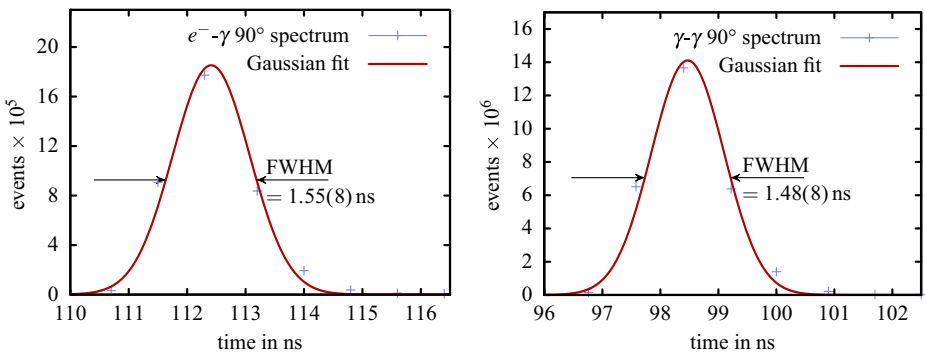


**Fig. 7** The prompt curve for the 553 keV–9.4 keV  $\gamma - \gamma$  coincidence detected with a CsF scintillation detector and an APD (right) and for the 17.8 keV–9.4 keV  $e^- - \gamma$  coincidence detected just with APDs. The deviation on the right side of the curve is due to the onset of the lifetime curve. Measurements uncertainties are smaller than the points indicate

is the dominant line in the  $^{83}\text{Rb}$  spectrum, see Fig. 5. The cascade’s initial level has a half-life of just 6.2(2.1) ps, thus the emission of the 553 keV  $\gamma$  and the X-ray can be considered simultaneous. The resulting spectrum and a Gaussian fit to the prompt line is shown in Fig. 7

on the right side. For the combination of scintillation detector and APD, the time resolution is 1.48(8) ns FWHM.

For the APD-only operation of the setup, the 17.8 keV conversion electron and the successively emitted 12.6 keV X-ray can be used to determine the time resolution. A resulting spectrum is shown in Fig. 7 on the left side. The width of the prompt curve is 1.55(8) ns FWHM.

## 4 Conclusions

Using the nuclei  $^{83}\text{Rb}$ ( $^{83}\text{Kr}$ ) and  $^{83\text{m}}\text{Kr}$ ( $^{83}\text{Kr}$ ) it is shown that PAC measurements using APDs and voltage sensitive amplifiers are feasible. An accurate measurement of the intermediate level's half-life is presented. With this small and simple set-up, a time resolution of 1.6 ns FWHM for the whole fast-slow apparatus is reached. This value is well comparable to the time resolution of a detector of type C30703 determined by Baron et al. [2]. The set-up proposed can easily be used for experiments with  $\gamma$  and conversion electron energies as low as 4.5 keV.

Furthermore, the usability of the nuclei  $^{83}\text{Rb}$ ( $^{83}\text{Kr}$ ) and  $^{83\text{m}}\text{Kr}$ ( $^{83}\text{Kr}$ ) as PAC probes has been shown.

**Acknowledgments** The help of A. D'Hein and S. Stahl during the development of the amplifier is greatly appreciated. Many thanks to A. Dahl, P.D. Eversheim, S. Hinderlich and C. Noll for taking care of the ion-implantations at the BONIS facility. We also like to thank our colleagues O. Lebeda, J. Sentkerestiová, M. Slezák and D. Vénos from NPI Řež for supplying the  $^{83}\text{Rb}$  activity.

Work partially funded by the BMBF Germany under contract number 05A14PDA and 05A11PD1.

## References

1. Kataoka, J., et al.: Recent progress of avalanche photodiodes in high-resolution X-rays and  $\gamma$ -rays detection. *Nucl. Instrum. Meth. A* **541**, 398–404 (2005). doi:[10.1016/j.nima.2005.01.081](https://doi.org/10.1016/j.nima.2005.01.081)
2. Baron, A.Q.R., Kishimoto, S., et al.: Silicon avalanche photodiodes for direct detection of X-rays. *J. Synchrotron Radiat.* **13**, 131–142 (2006). doi:[10.1107/S090904950503431X](https://doi.org/10.1107/S090904950503431X)
3. McCutchan, E.A.: Nuclear data sheets for  $A = 83$ . *Nucl. Data Sheets* **125**, 201–394 (2015). doi:[10.1016/j.nds.2015.02.002](https://doi.org/10.1016/j.nds.2015.02.002)
4. Kellö, V., Pyykkö, P., Sadlej, A.J.: Nuclear quadrupole moments of Kr and Xe from molecular data. *Chem. Phys. Lett.* **346**(1–2), 155–159 (2001). doi:[10.1016/S0009-2614\(01\)00940-X](https://doi.org/10.1016/S0009-2614(01)00940-X)
5. Baron, A.Q.R., Ruffer, R., Metge, J.: A fast, convenient, X-Ray detector. *Nucl. Instrum. Meth. A* **400**, 124–132 (1997). doi:[10.1016/S0168-9002\(97\)00936-4](https://doi.org/10.1016/S0168-9002(97)00936-4)
6. Flaxer, E.: A low-cost, ultra-fast and low-noise preamplifier for micro channel plates. *Meas. Sci. Technol.* **17**(8), 37–40 (2006). doi:[10.1088/0957-0233/17/8/N02](https://doi.org/10.1088/0957-0233/17/8/N02)
7. Arenz, M., Vianden, R.:  $^{83\text{m}}\text{Kr}$ , a potentially powerful PAC probe. *Hyperfine Interact.* **222**(1), 73–76 (2013). doi:[10.1007/s10751-012-0723-3](https://doi.org/10.1007/s10751-012-0723-3)
8. Vénos, D., Slezák, M., et al.: Gaseous source of  $^{83\text{m}}\text{Kr}$  conversion electrons for the neutrino experiment KATRIN. *J. Instrum.* **9**(12), P12010 (2014). doi:[10.1088/1748-0221/9/12/P12010](https://doi.org/10.1088/1748-0221/9/12/P12010)